Inorg. Chem. **2008**, *47*, 5666−5676

Generation of Blue Light-Emitting Zinc Complexes by Band-Gap Control of the Oxazolylphenolate Ligand System: Syntheses, Characterizations, and Organic Light Emitting Device Applications of 4-Coordinated Bis(2-oxazolylphenolate) Zinc(II) Complexes

Ho-Jin Son, Won-Sik Han, Ji-Yun Chun, Byoung-Kook Kang, Soon-Nam Kwon, Jaejung Ko,* Su Jung Han, Chongmok Lee, Sung Joo Kim, and Sang Ook Kang*

Department of Materials Chemistry, Korea University, 208 Seochang, Chochiwon, Chung-nam 339-700, South Korea, Department of Chemistry, Ewha Womans University, Seoul 120-750, South Korea, and Department of Materials Science and Engineering, Columbia University, New York 10027

Received December 24, 2007

Color-tunable Zn(II) complexes of the type Zn(*N,O*-OPh^{OxZ}ArX)$_2$ (**5**), where the ligand consists of an oxazolylphenolate ion connected at the 4-position by a 2,4-substituted aryl functional group with X = NMe_2 **a**, OMe **b**, Ph **c**, Cl **d**, F_2 **e**, and CN **f**, were prepared. X-ray structural studies of **5a**, **5b**, and **5e** showed that a zinc atom was positioned in a distorted tetrahedral coordination environment created by two oxazolylphenolate ligands with *N,O*-chelation. Hammet plots of absorption and emission maxima, respectively, in UV and photoluminescence (PL) spectra with respect to electron-donating and electron-withdrawing groups of the substituents indicate a direct correlation between the highest occupied molecular orbital (HOMO)−lowest unoccupied molecular orbital (LUMO) band gaps and electronic alterations at the ligand sites. A similar correlation was also observed for the reduction and oxidation potentials in cyclic voltammograms (CVs). A gradual increase in the HOMO−LUMO band gap is seen from electron-donating to electron-withdrawing functional groups, NMe_2 < OMe < Ph < Cl < F_2 < CN. An emission peak with a maximum at 455 nm was achieved when the most electron-withdrawing group (cyano) was applied to the oxazolylphenolate ligand system. Density-functional theory (DFT) calculations on the HOMOs and LUMOs for this series lead to a conclusion similar to that arrived at from a blue-shift trend observed in UV data and trends in the CVs. The 4-coordinated zinc complex (**5c**) was shown to be a potential blue-emitting material, exhibiting a maximum efficiency of 1720 cd/m^2 at 17 V with 0.3 cd/A in a multilayered device structure of ITO/NPB/**5c**/BCP/Alq_3/LiF/Al. On the basis of the low HOMO level of this series, **5a** was tested as a hole-transporting material; this resulted in the successful fabrication of a multilayered device of ITO/**5a**/DPVBI/Alq_3/LiF/Al with an efficiency of 7000 cd/m^2 at 13 V with 2.0 cd/A.

Introduction

Since the discovery of organic light emitting devices (OLEDs) by C. W. Tang[1] and J. H. Burroughes,[2] unrelenting efforts have been made to develop highly efficient electroluminescent (EL) materials. In particular, methods to construct blue light-emitting materials with large band gaps have long been sought; studies aimed at producing such materials have focused on small organic molecules and polymers. However, for the successful fabrication of full-color OLEDs, issues related to efficiency and lifetime of blue emitting materials need to be resolved. Major research on blue luminescent materials has been carried out mainly using aromatic organic molecules[3] and organic polymers.[4] Blue EL materials derived from organometallic complexes are rare and limited to late transition-metal complexes (Ir,[5] Pt,[6] Os[7]) and main group metal complexes[8,9] based on hydroquinoline-type ligands. For this reason, new types of organometallic EL materials utilizing main group metals (Al,[10] Be,[11] Cu,[12] Zn[13]) with *N,O*- and *N,N*-chelate ligands have been actively studied.

* To whom correspondence should be addressed. E-mail: sangok@korea.ac.kr. Tel: +82-41-860-1334. Fax: +82-41-867-5396.

(1) Tang, C. W.; VanSlyke, S. A. *Appl. Phys. Lett.* **1987**, *51*, 913.
(2) Burroughes, J. H.; Bradley, D. D. C.; Brown, A. R.; Marks, R. N.; Mackay, K.; Friend, R. H.; Burns, P. L.; Homes, A. B. *Nature* **1990**, *347*, 539.

10.1021/ic702491j CCC: $40.75
Published on Web 06/11/2008

Among them, zinc complexes have received much attention because of their many advantageous EL properties, such as electron transporting ability, light emitting efficiency, high thermal stability, ease of sublimation, and great diversity of tunable electronic properties resulting from ligand substitution.[13l–n,14] Because the electronic structure of metal chelate luminescent materials is determined by the coordination of a ligand, the coordination geometry as well as the highest occupied molecular orbital (HOMO) and the lowest unoccupied molecular orbital (LUMO) contributions from the ligand need to be examined. Indeed, the coordination mode of the ligand relates to the photophysical properties of the resulting metal complexes, and the bulkiness of the ligand alters the bonding around the metal center; a bulky ligand tends to form monomeric species while less bulky ligands encourage the formation of dimeric or trimeric metal complexes. Furthermore, modification of the chelating ligand in Alq_3 and Bq (q: hydroquinoline) with electron-donating or electron-withdrawing groups proves to be an effective method for the tuning of the optical properties of Alq_3[8] and Bq.[9b] However, until recently very few studies have been performed on the systematic tuning of the luminescence of zinc complexes. In an effort to investigate the efficacy of the substituent effect and its possible use in color tuning in zinc(II) complexes, a series of electron-rich and electron-poor oxazolylphenol ligands was prepared, and the resulting 4-coordinated Zn(oxazolylphenolate)$_2$ complexes were investigated for their electronic and photophysical properties.

Here, we report the full details of the syntheses and characterizations of various electron-donating and electron-withdrawing aryl-substituted Zn oxazolylphenolate complexes (**5**). The photophysical and electrochemical properties of these Zn complexes were estimated by means of UV and photoluminescence (PL) spectroscopy, as well as cyclic voltammetry (CV). The corresponding EL properties for **5a** and **5c** were studied through device fabrication by applying them respectively as hole-transporting and emitting materials in multilayer devices, depending on the HOMO and LUMO energy levels. In addition, theoretical calculations were performed to account for the change in the electronic structure as a result of the inductive and mesomeric effects on aryl substituents (ArX), as shown in Chart 1.

Results and Discussion

Synthesis of Zn[2-(5-aryl-2-hydroxyphenyl)oxazolate]$_2$ (5a−f). The synthesis strategy for the generation of oxazolylphenolate ligands (**4a−f**) is described in Scheme 1.

(3) (a) Higuchi, A.; Ohnishi, K.; Nomura, S.; Inada, H.; Shirota, Y. *J. Mater. Chem.* **1994**, *4*, 171. (b) Hosokawa, C.; Higashi, H.; Nakamura, H.; Kusumoto, T. *Appl. Phys. Lett.* **1995**, *67*, 3853. (c) Shirota, Y.; Ogawa, H.; Ohnishi, K. *Synth. Met.* **1997**, *91*, 243. (d) Zhang, Z.; Jiang, X.; Zhu, W.; Zhang, B.; Xu, S. *J. Phys. D: Appl. Phys.* **2001**, *34*, 3083. (e) Uchida, M.; Ono, Y.; Yokoi, H.; Nakano, T.; Furukawa, K. *J. Photopolym. Sci. Technol.* **2001**, *14*, 305.

(4) (a) Cho, H. N.; Kim, J. K.; Kim, D. Y.; Kim, C. Y.; Song, N. W.; Kim, D. *Macromolecules* **1999**, *32*, 1476. (b) Shimoda, H.; Kimura, M.; Miyashita, S.; Friend, R. H.; Burroughes, J. H.; Towns, C. R. *SID99 DIGEST* **1999**, 372.

(5) Brooks, J.; Babayan, Y.; Lamansky, S.; Djurovich, P. I.; Tsyba, I.; Bau, R.; Thompson, M. E. *Inorg. Chem.* **2002**, *41*, 3055.

(6) (a) Sajoto, T.; Djurovich, P. I.; Tamayo, A.; Yousufuddin, M.; Bau, R.; Thompson, M. E.; Holmes, R. J.; Forrest, S. R. *Inorg. Chem.* **2005**, *44*, 7992. (b) Liu, Q.-D.; Jia, W.-L.; Wang, S. *Inorg. Chem.* **2005**, *44*, 1332.

(7) Wu, P.-C.; Yu, J.-K.; Song, Y.-H.; Chi, Y.; Chou, P.-T.; Peng, S.-M.; Lee, G.-H. *Organometallics* **2003**, *22*, 4938.

(8) (a) Montes, V. A.; Pohl, R.; Shinar, J.; Anzenbacher, P., Jr *Chem.—Eur. J.* **2006**, *12*, 4523. (b) Lim, J. T.; Jeong, C. H.; Lee, J. H.; Yeom, G. Y.; Jeong, H. K.; Chai, S. Y.; Lee, I. M.; Lee, W. I. *J. Organomet. Chem.* **2006**, *691*, 2701. (c) Shi, Y.-W.; Shi, M.-M.; Huang, J.-C.; Chen, H.-Z.; Wang, M.; Liu, X.-D.; Ma, Y.-G.; Xu, H.; Yang, B. *Chem. Commun.* **2006**, 1941. (d) Meyers, A.; Weck, M. *Chem. Mater.* **2004**, *16*, 1183. (e) Cheng, J.-A.; Chen, C. H.; Liao, C. H. *Chem. Mater.* **2004**, *16*, 2862. (f) Montes, V. A.; Li, G.; Pohl, R.; Shinar, J.; Anzenbacher, P., Jr *Adv. Mater.* **2004**, *16*, 2001. (g) Pohl, R.; Montes, V. A.; Shinar, J.; Anzenbacher, P., Jr *J. Org. Chem.* **2004**, *69*, 1723. (h) Pohl, R.; Anzenbacher, P., Jr *Org. Lett.* **2003**, *5*, 2769. (i) Sapochak, L. S.; Padmaperuma, A.; Washton, N.; Endrino, F.; Schmett, G. T.; Marshall, J.; Fogarty, D.; Burrows, P. E.; Forrest, S. R. *J. Am. Chem. Soc.* **2001**, *123*, 6300. (j) Chen, C. H.; Shi, J. M. *Coord. Chem. Rev.* **1998**, *171*, 161. (k) Matsumura, M.; Akai, T. *Jpn. J. Appl. Phys., Part 1* **1996**, *35*, 5357. (l) Hopkins, T. A.; Meerholz, K.; Shaheen, S.; Anderson, M. L.; Schmidt, A.; Kippelen, B.; Padias, A. B.; Hall, H. K., Jr; Peyghambarian, N.; Armstrong, N. R. *Chem. Mater.* **1996**, *8*, 344.

(9) (a) Wang, J.; Oyler, K. D.; Bernhard, S. *Inorg. Chem.* **2007**, *46*, 5700. (b) Qin, Y.; Kiburu, I.; Shah, S.; Jäkle, F. *Org. Lett.* **2006**, *8*, 5227. (c) Garon, S.; Lau, E. K. C.; Chew, S.-L.; Lee, S. T.; Thompson, M. E. *Journal of the SID* **2005**, *13*, 405. (d) Mishra, A.; Periasamy, N.; Patankar, M. P.; Narasimhan, K. L. *Dyes Pigm.* **2005**, *66*, 89. (e) Jaafari, A.; Ouzeau, V.; Ely, M.; Rodriguez, F.; Yassar, A.; Aaron, J. J.; Benalloul, P.; Barthou, C. *Synth. Met.* **2004**, *147*, 175. (f) Wang, G.; Liang, F.; Xie, Z.; Su, G.; Wang, L.; Jing, X.; Wang, F. *Synth. Met.* **2002**, *131*, 1. (g) Leung, L. M.; Lo, W. Y.; So, S. K.; Lee, K. M.; Choi, W. K. *J. Am. Chem. Soc.* **2000**, *122*, 5640. (h) Tao, X. T.; Suzuki, H.; Wada, T.; Miyata, S.; Sasabe, H. *J. Am. Chem. Soc.* **1999**, *121*, 9447. (i) Curioni, A.; Boero, M.; Andreoni, W. *Chem. Phys. Lett.* **1998**, *294*, 263. (j) Kido, J.; Iizumi, Y. *Chem. Lett.* **1997**, 963. (k) Burrows, P. E.; Shen, Z.; Bulovic, V.; McCarty, D. M.; Forrest, S. R.; Cronin, J. A.; Thompson, M. E. *J. Appl. Phys.* **1996**, *79*, 7991.

(10) (a) Wang, J. F.; Jabbour, G. E.; Mash, E. A.; Anderson, J.; Zhang, Y. D.; Lee, P. A.; Armstrong, N. R.; Peyghambarian, N.; Kippelen, B. *Adv. Mater.* **1999**, *11*, 1266. (b) Liu, X.; Xia, H.; Gao, W.; Ye, L.; Mu, Y.; Su, Q.; Ren, Y. *Eur. J. Inorg. Chem.* **2006**, 1216.

(11) (a) Tong, Y.-P.; Zheng, S.-L.; Chen, X.-M. *Inorg. Chem.* **2005**, *44*, 4270. (b) Hu, N.-X.; Esteghamation, M.; Xie, S.; Popovic, Z.; Hor, A.-M.; Ong, B.; Wang, S. *Adv. Mater.* **1999**, *11*, 1460. (c) Hamada, Y.; Sano, T.; Fujita, M.; Fujii, T.; Nishio, Y.; Shibata, K. *Chem. Lett.* **1993**, 905.

(12) (a) Zhao, S.-B.; Wang, R.-Y.; Wang, S. *Inorg. Chem.* **2006**, *45*, 5830. (b) McCormick, T.; Jia, W.-L.; Wang, S. *Inorg. Chem.* **2006**, *45*, 147. (c) Jia, W. L.; McCormick, T.; Tao, Y.; Lu, J.-P.; Wang, S. *Inorg. Chem.* **2005**, *44*, 5706. (d) Zhang, Q.; Zhou, Q.; Cheng, Y.; Wang, L.; Ma, D.; Jing, X.; Wang, F. *Adv. Mater.* **2004**, *16*, 432. (e) Cuttell, D. G.; Kuang, S. M.; Fanwick, P. E.; McMillin, D. R.; Walton, R. A. *J. Am. Chem. Soc.* **2002**, *124*, 6. (f) Ma, Y.; Che, C.-M.; Chao, H.-Y.; Zhou, X.; Chan, W.-H.; Shen, J. *Adv. Mater.* **1999**, *11*, 852.

(13) (a) Xu, X.; Liao, Y.; Yu, G.; You, H.; Di, C.; Su, Z.; Ma, D.; Wang, Q.; Li, S.; Wang, S.; Ye, J.; Liu, Y. *Chem. Mater.* **2007**, *19*, 1740. (b) Gorner, H.; Khanra, S.; Weyhermuller, T.; Chaudhuri, P. *J. Phys. Chem. A* **2006**, *110*, 2587. (c) Zhang, J.; Gao, S.; Che, C.-M. *Eur. J. Inorg. Chem.* **2004**, 956. (d) Liu, Q.-D.; Wang, R.; Wang, S. *Dalton Trans.* **2004**, 2073. (e) Yu, G.; Yin, S.; Liu, Y.; Shuai, Z.; Zhu, D. *J. Am. Chem. Soc.* **2003**, *125*, 14816. (f) Wang, P.; Hong, Z.; Xie, Z.; Tong, S.; Wong, O.; Lee, C.-S.; Wong, N.; Hung, L.; Lee, S. *Chem. Commun.* **2003**, 1664. (g) Kim, T. S.; Okubo, T.; Mitani, T. *Chem. Mater.* **2003**, *15*, 4949. (h) Sapochak, L. S.; Benincasa, F. E.; Schofield, R. S.; Baker, J. L.; Riccio, K. K. C.; Fogarty, D.; Kohlmann, H.; Ferris, K. F.; Burrows, P. E. *J. Am. Chem. Soc.* **2002**, *124*, 6119. (i) Pang, J.; Marcotte, Eric J.-P.; Seward, C.; Stephan Brown, R.; Wang, S. *Angew. Chem., Int. Ed.* **2001**, *40*, 4042. (j) Wang, S. *Coord. Chem. Rev.* **2001**, *215*, 79. (k) Hamada, Y.; Sano, T.; Fujii, H.; Nishio, Y.; Takahashi, H.; Shibata, K. *Jpn. J. Appl. Phys.* **1996**, *35*, 1339. (l) Yang, W.; Schmider, H.; Wu, Q.; Zhang, Y.-S.; Wang, S. *Inorg. Chem.* **2000**, *39*, 2397. (m) Hopkins, T. A.; Meerholz, K.; Shaheen, S.; Anderson, M. L.; Schmidt, A.; Kippelen, B.; Padias, A. B.; Hall, H. K., Jr; Peyghambarian, N.; Armstrong, N. R. *Chem. Mater.* **1996**, *8*, 344. (n) Nakamura, N.; Wakabayashi, S.; Miyairi, K.; Fujii, T. *Chem. Lett.* **1994**, 1741.

(14) (a) Kijima, Y.; Asai, N.; Kishii, N.; Tamura, S.-I. *IEEE J. Quantum Electron.* **1998**, *4*, 40. (b) Hamada, Y. *IEEE Trans. Electron Devices* **1997**, *44*, 1208.

Chart 1. Zn Complexes Containing Electron-Donating/Withdrawing Groups (**5**)

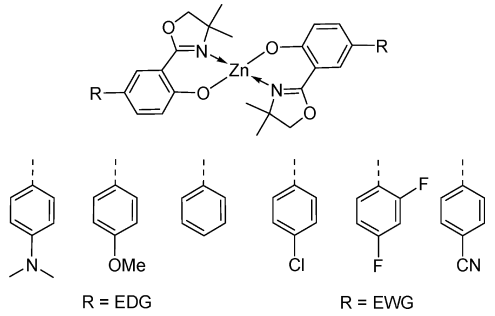

Oxazolyl-4-bromophenol (**1**) was prepared from the corresponding aminoalcohol and carboxylic acid in moderate yields, using a previously developed synthesis protocol.[15] Subsequent protection of the phenolic oxygen atom was carried out by reacting **1** with benzyl chloride in the presence of base. A series of Suzuki-type cross-coupling reactions were successfully performed to yield the desired oxazolylphenolate ligands (**3**) with suitable handling of electron-donating and electron-withdrawing functional groups in the para position. The final oxazolylphenol ligands (**4**) were obtained using a hydrogenolytic deprotection procedure, as shown in Scheme 1.

Zn(II) complexes of Zn(*N,O*-OPh^{OxZ}ArX)$_2$ were obtained by reacting 2 equiv of ligand **4** with Zn(OAc)$_2$ in ethanol (Scheme 1). In all cases, products were isolated from the reaction solution by slow recrystallization. After recrystallization, filtration followed by washing with cold ethanol resulted in the production of crude products in moderate yields. The formation of metal complex **5** was confirmed by means of high-resolution mass spectrometry and elemental analyses. All Zn(II) complexes showed the expected signals in the ^{1}H and ^{13}C NMR spectra, confirming the ligand coordination (see Experimental Section).

X-ray Structural Studies on Zn(*N, O*-OPh^{OxZ}ArX)$_2$, 5a, 5b, and 5e. Structural studies on **5a**, **5b**, and **5e** showed that the zinc atom resides in a tetrahedral coordination site as a monomeric entity. Oak Ridge Thermal Ellipsoid Plot (ORTEP) structures of **5a**, **5b**, and **5e** are shown in Figures 1–3, and X-ray structural parameters, selected bond lengths, and angles are presented in Tables 1 and 2, respectively. The dimethyl units on the oxazolyl group provide steric protection against further metal coordination from nearby zinc atoms. In general, most anhydrous zinc complexes with a hydroxyquinolinate ligand exist as tetramers[13a,c,e,h] or hexamers[13g] because the ligand has a planar structure ensuring there are no bulky substituents near the nitrogen and oxygen atoms to interfere with metal coordination. The zinc(II) ion in each complex of **5a**, **5b**, and **5e** is symmetrically coordinated to two *N,O*-chelate ligands with an N→Zn−O conformation. Therefore, all four structures adopt a pseudotetrahedral geometry different from that found in tetrameric zinc complexes, a distorted trigonal bipyramidal geometry. The Zn−O and Zn−N lengths are in the range of 1.906−1.921 Å and 1.975−1.988 Å, implying the presence of regular σ and dative bonding, respectively (Table 2). When compared with the bond lengths of tetrameric zinc complexes of Zn−O (1.962−2.058 Å) and Zn−N (2.095−2.170 Å), these values are shorter because of the effective coordination by the *N,O*-chelating oxazolylphenolate ligand (**4**). This again reflects the preference for 4-coordination by the oxazolylphenolate ligand system studied in this work. It is noteworthy that the Zn−O bond length in a series varies depending on the electron-donating and electron-withdrawing substituents: the bond length decreases from 1.9203(14) Å for **5a** to 1.906(4) Å for **5e**. The angles around a zinc atom deviate substantially from the tetrahedral values, exhibiting bond angles of 120.4(2)−124.39(7)° and 114.7(3)−116.96(6)° for N−Zn−N and O−Zn−O, respectively. One special feature common to all three structures is that intermolecular π-π interactions are discernible in the crystal packings, especially in the aryl periphery. Shorter intermolecular distances of 3.665−3.745 Å were found in aryl-aryl stacking regions of **5a**, **5b**, and **5e**, which is typical of aromatic−aromatic face-to-face π-π stacking.[16] Figure 4 shows a molecular packing view of **5a**, **5b**, and **5e**. Such an increase in intermolecular interaction can be suggested as an origin of the high carrier mobility in EL devices.

Photophysical Properties. The UV−visible absorption and fluorescence spectra of the ligand-functionalized Zn complexes (**5**) are summarized in Table 3 and Figures 5–7).

Scheme 1. Preparation of Zn Complexes (**5**)

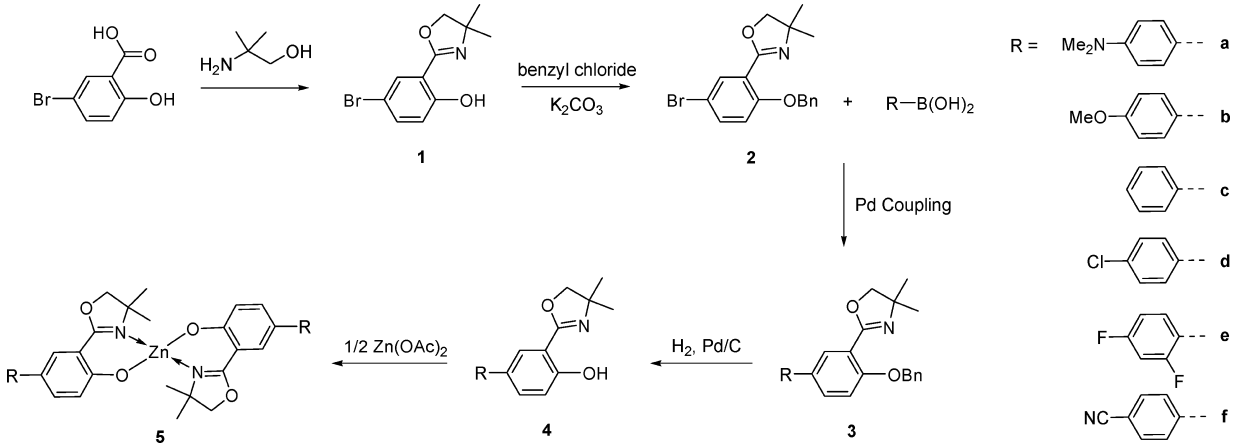

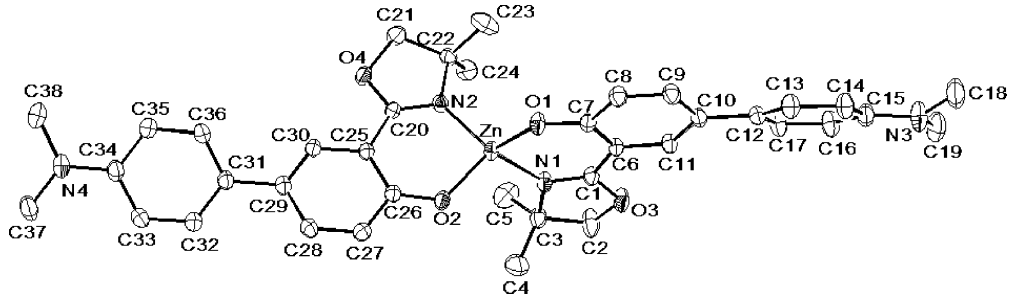

Figure 1. ORTEP drawing (30% probability for thermal ellipsoids) of **5a**. Hydrogen atoms are omitted for clarity.

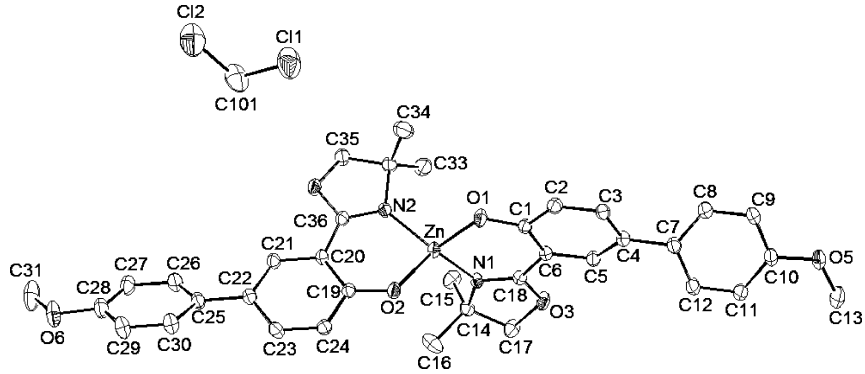

Figure 2. ORTEP drawing (30% probability for thermal ellipsoids) of **5b**. Hydrogen atoms are omitted for clarity.

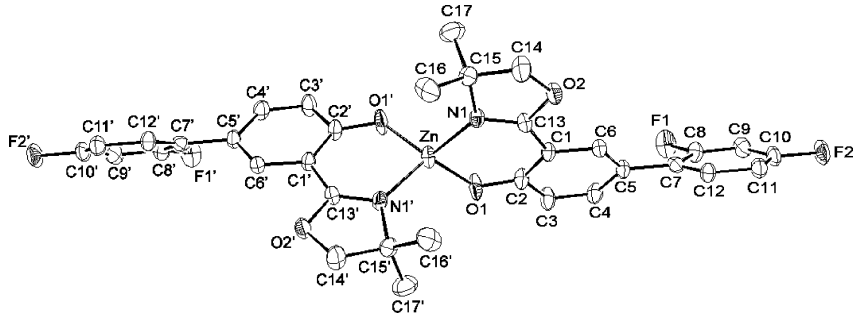

Figure 3. ORTEP drawing (30% probability for thermal ellipsoids) of **5e**. Hydrogen atoms are omitted for clarity.

Table 1. Crystal Data and Structure Refinement for **5a**, **5b**, and **5e**[a,b]

	5a	5b	5e
empirical formula	$C_{38}H_{42}N_4O_4Zn$	$C_{36}H_{36}N_2O_6Zn \cdot CH_2Cl_2$	$C_{34}H_{28}F_4N_2O_4Zn$
formula weight	684.13	742.96	669.95
temperature	233(2) K	233(2) K	233(2) K
wavelength	0.71073 Å	0.71073 Å	0.71073 Å
crystal system, space group	triclinic, $P\bar{1}$	triclinic, $P\bar{1}$	monoclinic, $P2/c$
unit cell dimensions	$a = 7.645(2)$ Å, $\alpha = 73.477(4)°$	$a = 7.589(2)$ Å, $\alpha = 76.161(5)°$	$a = 15.244(2)$ Å, $\alpha = 90°$
	$b = 12.213(3)$ Å, $\beta = 79.463(4)°$	$b = 13.137(3)$ Å, $\beta = 80.499(5)°$	$b = 6.6431(7)$ Å, $\beta = 103.071(2)°$
	$c = 19.148(4)$ Å, $\gamma = 88.053(4)°$	$c = 19.121(4)$ Å, $\gamma = 75.500(4)°$	$c = 15.110(2)$ Å, $\gamma = 90°$
volume	1684.9(6) Å^3	1780.6(7) Å^3	1490.5(3) Å^3
Z, calculated density	2, 1.348 mg/m^3	2, 1.386 mg/m^3	2, 1.488 mg/m^3
reflections collected/unique	23308/8409 [R(int) = 0.0239]	24442/8785 [R(int) = 0.0412]	14657/3704 [R(int) = 0.1063]
final R indices [$I > 2\sigma(I)$]	$R_1 = 0.0373$, $wR_2 = 0.1037$	$R_1 = 0.0440$, $wR_2 = 0.1086$	$R_1 = 0.0637$, $wR_2 = 0.1562$
R indices (all data)	$R_1 = 0.0517$, $wR_2 = 0.1158$	$R_1 = 0.0831$, $wR_2 = 0.1339$	$R_1 = 0.1692$, $wR_2 = 0.2269$

[a] $R_1 = \sum||F_o| - |F_c||$ (based on reflections with $F_o^2 > 2\sigma F^2$). [b] $wR_2 = [\sum[w(F_o^2 - F_c^2)^2]/\sum[w(F_o^2)^2]]^{1/2}$; $w = 1/[\sigma^2(F_o^2) + (0.095P)^2]$; $P = [\max(F_o^2, 0) + 2F_c^2]/3$ (also with $F_o^2 > 2\sigma F^2$).

In this series, we observed a correlation between the photophysical properties and the electronic nature of the attached substituents. A systematic blue-shift on both the absorption and emission spectra is observed on going from electron-donating to electron-withdrawing substituents of the modulator group. This, in turn, provides evidence of an electronic communication between the oxazolylphenolate fluorophores and the appended moieties. It is noteworthy that compound **5f** does not follow the trend in the series. Photophysical properties of **5a**-**f** shown in Table 3 reveal that the fluorescence quantum yield correlates with the electronic nature of the ligands. For the complexes bearing electron-withdrawing substituents, the quantum yield was increased, whereas the electron-rich moiety resulted in a decrease in the emission

Table 2. Selected Bond Lengths and Angles of **5a**, **5b**, and **5e**

structure parameter[a]	5a	5b	5e
Zn−O(1)	1.920(1)	1.921(2)	1.906(4)
Zn−O(2)	1.920(1)	1.920(2)	1.906(4)
Zn−N(1)	1.987(2)	1.977(2)	1.975(4)
Zn−N(2)	1.988(2)	1.975(2)	1.975(4)
O(1)−Zn−O(2)	116.96(6)	115.30(8)	114.7(3)
N(1)−Zn−N(2)	124.39(7)	123.91(9)	120.4(2)
N(1)−Zn−O(2)	111.34(7)	115.18(8)	117.2(2)
O(1)−Zn−N(1)	94.91(6)	95.42(8)	94.6(2)
O(1)−Zn−N(2)	116.08(6)	113.85(8)	117.2(2)
N(2)−Zn−O(2)	94.81(6)	94.70(8)	94.6(2)
dihedral angle[b]	22.2(3)	33.2(4)	47.3(8)

[a] Bond lengths are reported in angstroms and bond angles in degrees. [b] C(9)−C(10)−C(12)−C(17) for **5a**, C(3)−C(4)−C(7)−C(8) for **5b**, and C(4)−C(5)−C(7)−C(8) for **5e**.

quantum yield. This correlates well with the energy-gap law, suggesting a uniform nature of photophysical behavior in the series of complexes.

X-ray crystallographic structure determinations for **5a**, **5b**, and **5e** suggest that there is a higher degree of coplanarity for the electron-donating derivatives than for the electron-withdrawing compound. In particular, compound **5e** displays a 47.4° dihedral angle between the planes of phenol and the phenyl groups, whereas the dihedral angles for **5a** and **5b** are 22.2 and 32.2°, respectively. This may provide additional information on a blue-shift trend of the electron-poor systems found in both UV and fluorescence spectra. It is worthy of note that the crystal packing geometries of **5a**, **5b**, and **5e** show strong intermolecular π-π stacking between the modulator phenyl rings. This relates to an enhanced red-shifted trend for the film fluorescent spectra found in Table 3.

Electrochemistry. The electrochemical properties of zinc complexes containing two oxazolylphenolate ligands (**5**) were investigated by cyclic voltammetry (CV). The CV results are summarized in Table 4 using CH_3CN containing 0.1 M tetrabutylammonium hexafluorophosphate ($TBAPF_6$) with a scan rate of 0.1 V s^{-1}, and are also shown in Supporting Information, Figure S4. The potential values of the first redox wave in the scan of both the positive (E_{ox}) and negative (E_{red}) directions are included in Table 4, along with some multiple redox waves.

It is notable that characteristic redox properties are discernible with respect to electron-donating and electron-withdrawing substituents at the 2,4-position of the aryl substituent ring. The CVs of **5a** and **5b** show two oxidation waves in the positive potential range because electron-donating substituents provide electrons to the compound upon oxidation, which in turn stabilize the radical cation (Supporting Information, Figure S4a,b). The CVs of **5e** and **5f** exhibit one or two reversible reduction waves in the negative potential range because electron-poor substituents can accommodate electrons upon reduction to form stable anion radicals (Supporting Information, Figure S4e,f). These explanations are strongly supported by Hammett plots of the E_{ox} and E_{red} values versus σ values of the substituents, where a good linear relationship is observed based on the electron-donating/withdrawing substituents on the arylphenolate ring (Figure 8).

When an electrochemistry of the free ligand **4a** was carried out in CH_3CN, one reversible oxidation peak and one irreversible reduction peak were discernible in the corresponding CV (see Supporting Information, Figure S4a). The peak separation of the oxidation waves due to ligand **4a** in the CV of **5a** is more pronounced on changing the solvent from CH_3CN to CH_2Cl_2/CH_3CN (v/v = 4/1), which might be ascribed to electronic communication between the two ligand centers as a result of significant charge delocalization (Figure 9).[17]

The E_{ox} and E_{red} values are known to be related to the HOMO and LUMO energy levels, respectively. The HOMO and LUMO energy levels for the Zn(II) complexes (**5**) shown in Table 4 were calculated based on the relationship HOMO/LUMO (eV) = $-e(E_{ox}/E_{red}$ (V vs SCE) + 4.74 V).[18] The HOMO and LUMO energy levels of **5** were estimated to be about −5.89 to about −5.28 eV and about −2.27 to about −2.57 eV, respectively. Overall, the HOMO levels decrease systematically on going from electron-rich to electron-poor substituents, whereas the LUMO levels are less sensitive to ligand variation, with a deviation of ∼Δ 0.3 eV. This result correlates well with the blue shift in the UV spectra (Figure 12). Plots of the absorption maximum wavenumber υ_{abs} and emission maximum wavenumber υ_{em} versus ΔE (= E_{ox} − E_{red}) showed a direct correlation between HOMO−LUMO band gaps and electronic alteration from the ligand sites (Figure 10). A linear relationship was obtained between υ_{abs} and ΔE ($\upsilon_{abs} \times 10^4 = 1.764 + 0.303\Delta E$) except for **5f**, and the linearity for υ_{em} showed a relatively high slope ($\upsilon_{em} \times 10^4 = -0.606 + 0.896\Delta E$). The origin of the discrepancy of the band gap of **5f** between from absorption spectrum and from electrochemistry is uncertain at this moment. However, it is noticeable that the absorption spectrum of **5f** has a shoulder peak at 370 nm unlike other **5** compounds.

Theoretical Studies of Zn Complexes (5). To investigate the nature of the electronic structure, quantum chemical calculations of a series of Zn complexes (**5**) using density-functional theory (DFT) as implemented in the DMol^3 package were carried out.[19] The HOMO−LUMO levels of **5** were calculated using double numerical plus d-functions (DND), and the geometries were optimized under the same conditions. No atom was omitted from the detailed study of the bond lengths and angles of the optimized structure. Previous work on Zn(II) chelate $[Zn(L)_2]_n$ complexes (n = 1 or 2) has shown that the electron density of the HOMO is localized mainly on the phenoxide ring while the LUMO is localized on the heterocyclic ring.[13a,e,h] A similar result is observed in our calculation: the HOMO orbitals of $Zn(Oxa)_2$

(15) Hoveyda, H. R.; Karunaratne, V.; Rettig, S. J.; Orvig, C. *Inorg. Chem.* **1992**, *31*, 5408.
(16) Roesky, H. W.; Andruh, M. *Coord. Chem. Rev.* **2003**, *236*, 91.
(17) Barrière, F.; Geiger, W. E. *J. Am. Chem. Soc.* **2006**, *128*, 3980.
(18) Bard, A. J. ; Faulkner, L. R. In *Electrochemical Methods: Fundamentals and Applications*, 2nd ed.; John Wiley & Sons, Inc.: 2001; p 54.
(19) (a) Delley, B. *J. Chem. Phys.* **1990**, *92*, 508. (b) Delley, B. *J. Chem. Phys.* **2000**, *113*, 7756.
(20) (a) *SMART and SAINT*; Bruker Analytical X-ray Division: Madison, WI, 2002. (b) Sheldrick, G. M. *SHELXTL-PLUS Software Package*; Bruker Analytical X-ray Division: Madison, WI, 2002.

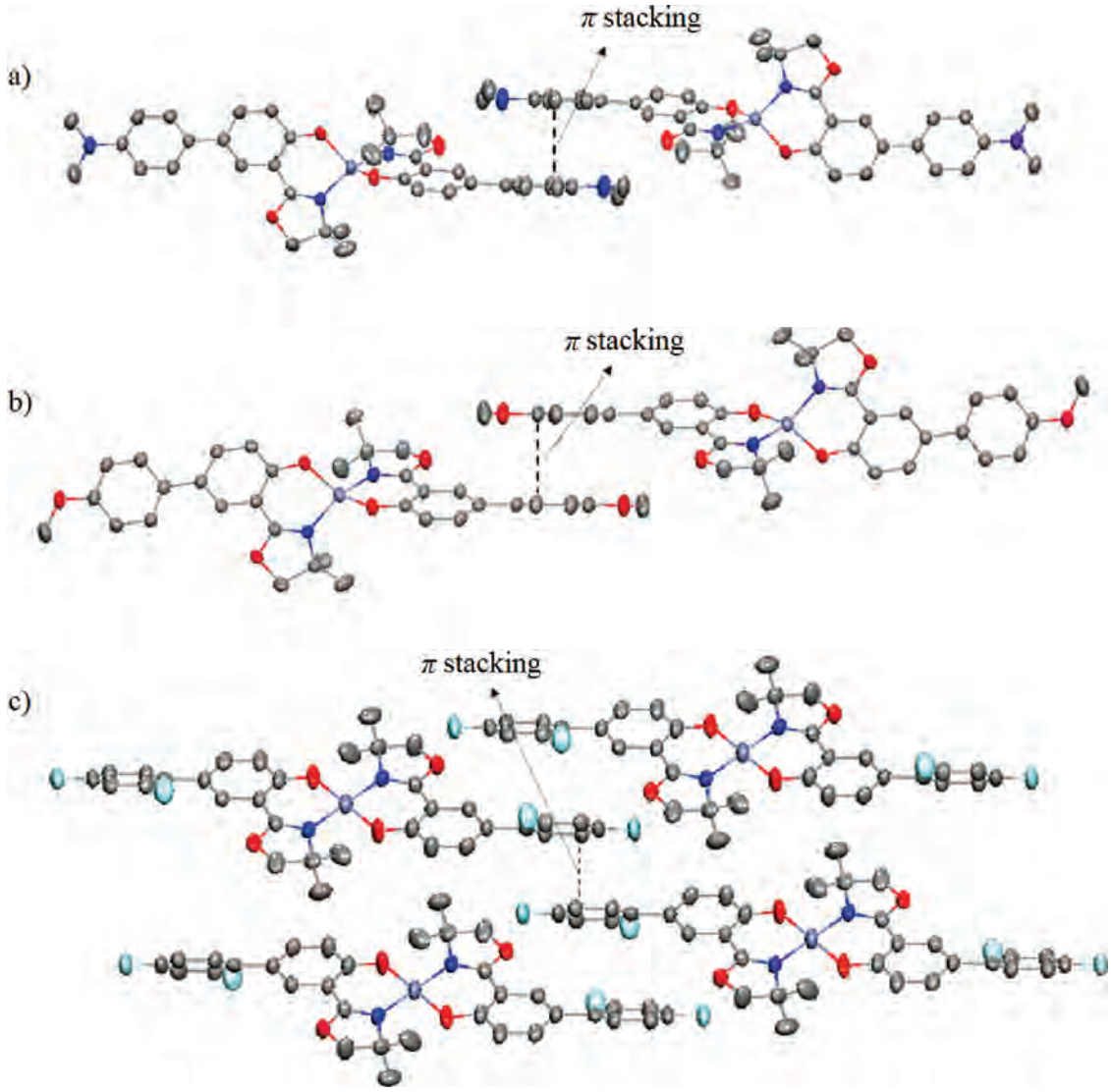

Figure 4. Packing diagram showing the intermolecular π-π interaction of **5a** (a), **5b** (b), and **5e** (c).

Table 3. UV-vis, Photoluminescence Spectra, And Thermal Data for **5**

	UV−vis (nm)		PL (nm)			
compounds	solution[a]	film[b]	solution[a]	film[b]	Φ_f (%)[c]	M_p (°C)
5a	372	382	482	486	2	334
5b	369	374	440	465	11	340
5c	363	369	428	463	8	327
5d	362	367	423	462	10	355
5e	357	360	420	449	16	324
5f	326	327	416	455	12	368

[a] In chloroform. [b] In thin solid film. [c] Relative to 9,10-diphenylanthracene in chloroform at ambient temperature.

are distributed over a phenoxide and substituted aryl rings, whereas the LUMO orbitals are located on phenoxide and oxazolyl rings (see Supporting Information, Figure S5). From these data, HOMO and LUMO energies are assumed to be dominated by orbitals originating from the 2-(5-aryl-2-hydroxyphenyl)oxazoline ligands in all cases where the contributions of core metal Zn(II) are almost negligible. In addition, there was a smooth decrease in both HOMO and LUMO energy levels of the six model compounds, showing a similar result with relatively constant LUMO levels obtained in the CV experiments (Figure 11).

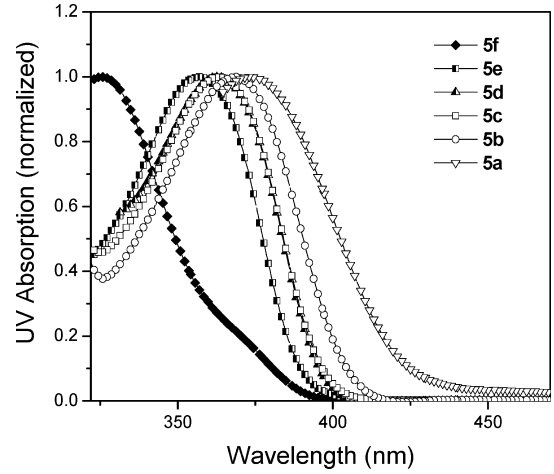

Figure 5. UV−vis absorption spectra of **5** in chloroform.

Fabrication of OLED Devices. On the basis of the HOMO and LUMO energy levels obtained by CV, **5c** was selected as a reference to compare the results reported in a similar study.[13g,h,k] Devices for the emitting and electron-transporting layer were fabricated with the structure ITO/

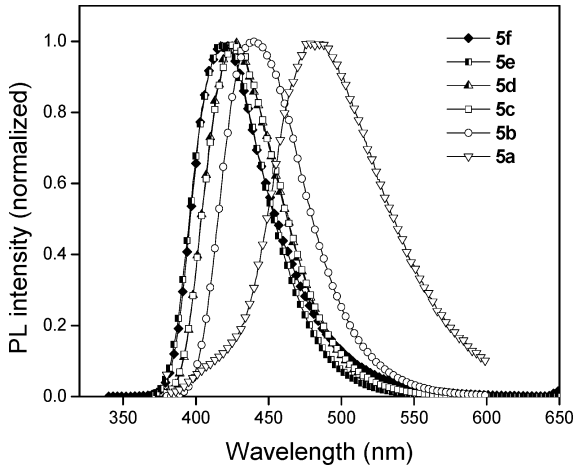

Figure 6. PL spectra of **5** in chloroform.

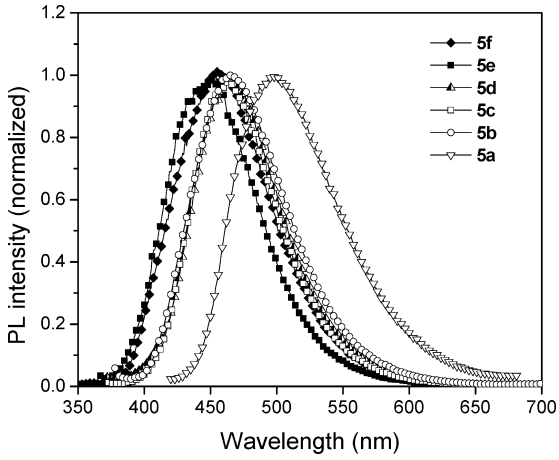

Figure 7. PL spectra of **5** in a solid film.

NPB/**5c**/LiF/Al (Table 5). However, the brightness and efficiency turned out to be relatively poor, indicating the difficulty of electron injection from the cathode. For this reason, the device structure ITO/NPB/**5c**/Alq_3/LiF/Al using Alq_3 as an electron-transporting layer was tested. As shown in Supporting Information, Figure S6, the device showed improved efficiency and brightness. However, the EL peak showed interference from the Alq_3 color that demonstrated the recombination of holes and electrons in the Alq_3 layer due to the low HOMO level of **5c** (Supporting Information, Figure S7). To solve this problem, 2,9-dimethyl-4,7-diphenylphenanthroline (**BCP**) was inserted into the device as a hole-blocking layer. As expected, the EL peak of the device (ITO/NPB/**5c**/BCP/Alq_3/LiF/Al) showed agreement with the film PL of **5c** that proved exciton formation in the **5c** layer, displaying a maximum brightness of 1720 cd/cm^2 at 17 V and a current efficiency of 0.3 cd/A at 2 mA/cm^2. In addition, we found that **5a** can be applied as a hole transporting layer (HTL) on the basis of the preliminary HOMO/LUMO levels determined by CV (Figure 12). Because **5a** has two reversible oxidation peaks in the CV, a hole from the anode can be stabilized in these two electronic states. Accordingly, a device was fabricated with the structure ITO/**5a**/DPVBI/Alq_3/LiF/Al and another device of structure ITO/NPB/DPVBI/Alq_3/LiF/Al was fabricated as a reference. As shown in Figure 13, the former device displayed a maximum brightness of 7000 cd/cm^2 at 13 V and a maximum current efficiency of 2.0 cd/A at 3 mA/cm^2, showing the potential of **5a** as a hole-transporting material.

Conclusion

To carry out a systematic study of Zn(II) complexes, we prepared metal chelating complexes based on new types of ligand systems. The structures of monomeric Zn(II) complexes [$Zn(L)_2$] were characterized by X-ray analyses. This showed that ligand bulkiness is closely related to intermolecular interaction. From photophysical and electrochemical studies, we found that the band gap and HOMO/LUMO levels of the prepared Zn(II) complexes can be efficiently controlled by electron-donating and -withdrawing substituents on the ligands. In particular, fabrication of devices using **5c** and **5a** showed the potential of these compounds as a blue luminescent material and a hole-transporting material, respectively. This method offers a powerful tool for the preparation of electroluminescent material using a metal complex with a chelating ligand.

Experimental Section

General Procedures. All manipulations were performed under a dry nitrogen (or argon) atmosphere using standard Schlenk techniques. Tetrahydrofuran (THF) was freshly distilled over potassium benzophenone. ^{1}H and ^{13}C spectra were recorded on a Varian Unity Inova AS600 spectrometer operating at 599.80 and 150.83 MHz, respectively. All proton and carbon chemical shifts were measured relative to internal residual benzene from the lock solvent (99.9% $CDCl_3$) and then referenced to Me_4Si (0.00 ppm). Elemental analyses were performed with a Carlo Erba Instruments CHNS-O EA 1108 analyzer. High Resolution Tandem Mass Spectrometry (Jeol LTD JMS-HX 110/110A) was performed by the Korean Basic Science Institute (Seoul). Absorption and photoluminescence spectra were recorded on a SHIMADZU UV-3101PC UV−vis−NIR scanning spectrophotometer and a VARIAN Cary Eclipse fluorescence spectrophotometer, respectively. The fluorescence quantum yields in chloroform using 9,10-diphenylanthracene as a standard were determined by the dilution method. CV experiments were carried out in CH_3CN or CH_2Cl_2/CH_3CN (v/v = 4/1) mixed solution containing electro-active compounds and 0.1 M tetrabutylammonium hexafluorophosphate ($TBAPF_6$, or 0.1 M tetrabutylammonium tetrafluoroborate ($TBABF_4$)) at room temperature using a BAS 100B electrochemical analyzer. A glassy carbon disk (Φ = 3 mm, or platinum disk (Φ = 1.6 mm)), platinum wire, and Ag|$AgNO_3$ (0.1 M) were used as the working, counter, and reference electrodes, respectively. All potential values were calibrated versus the ferrocene/ferrocenium ($Fc|Fc^+$) redox couple, and then corrected to the saturated calomel electrode (SCE) on the basis of an $Fc|Fc^+$ redox potential of 0.38 V versus SCE. Zinc(II) acetate, 2-amino-2-methyl-1-propanol, 5-bromo salicylic acid, and palladium(II) acetate were purchased from Aldrich. Materials (**5**) were purified by train sublimator (DOV Sublimation system model-DOV1200) prior to device fabrication. ITO-coated glass (20 Ω/sq) was first cleaned by conventional procedures. Under an inert atmosphere in a fabrication chamber, the sample was exposed to UV/ozone treatment. Then, organic and metal layers were deposited thermally onto the ITO surface at a rate of 1∼2 Å/s at a pressure of about 4 × 10^{-6} Torr. Typical devices were fabricated with NPB or **5a** as the hole-transporting layer (HTL, 50 nm), **5c** or DPVBI

Table 4. Cyclic Voltammetric Data and Theoretical Data of Zn Complexes[a]

	oxidation [V][b]		reduction [V][b]		[eV]		
compound	E_{pa1} (E_{pa2})	E_{pc1} (E_{pc2})	E_{pa1} (E_{pa2})	E_{pc1} (E_{pc2})	E_g[e]	HOMO[d]	LUMO[d]
5a	+0.57 (+0.84)	+0.51 (+0.79)	*c*	−2.50	3.01	−5.28	−2.27
5b	+0.98 (+1.32)	+0.89	*c*	−2.31	3.20	−5.68	−2.48
5c	+1.07	*c*	−2.26	−2.31	3.33	−5.78	−2.45
5d	+1.09	*c*	*c*	−2.24	3.27	−5.80	−2.53
5e	+1.14	*c*	−2.24	−2.29	3.37	−5.85	−2.48
5f	+1.18	*c*	*c* (−2.36)	−2.21 (−2.45)	3.32	−5.89	−2.57

[a] CVs were recorded at room temperature in CH_3CN/0.1 M $TBAPF_6$. [b] E_{ox} and E_{red} are represented as E_{pa} and E_{pc} (V vs SCE). [c] It is hard to measure this value because of the lack of reversibility. [d] HOMO and LUMO levels were determined using the following equations: E_{HOMO} (eV) $= -e(E_{ox} + 4.74)$, E_{LUMO} (eV) $= -e(E_{red} + 4.74)$. [e] E_g = LUMO − HOMO.

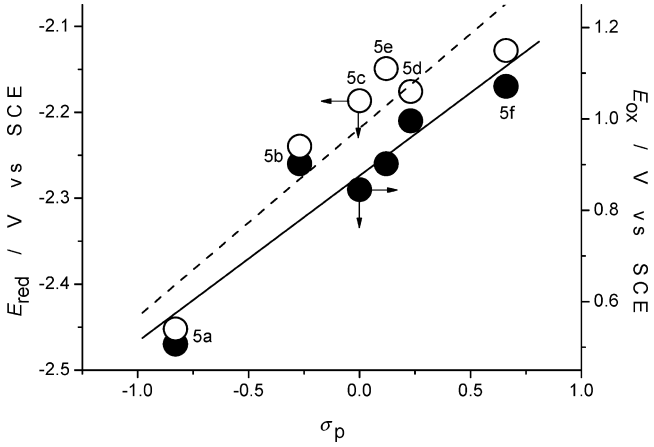

Figure 8. Plots of reduction (open circle, dashed line) and oxidation (closed circle, solid line) peak potentials as a function of the σ_p values of para-substituents on the phenyl groups of **5**.

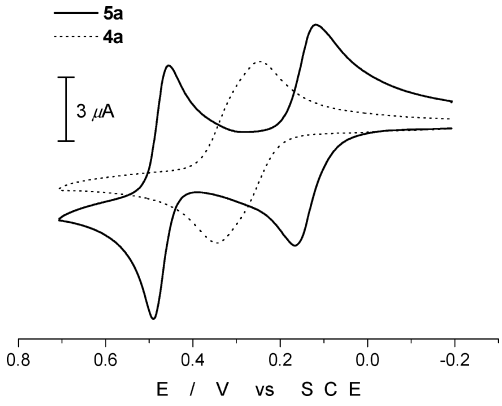

Figure 9. Cyclic voltammograms of 0.5 mM **5a** (solid line) and **4a** (dashed line). The peaks were examined at a platinum electrode ($\Phi = 1.6$ mm) in 4:1 (*v*/*v*) CH_2Cl_2/CH_3CN solution containing 0.1 M $TBABF_4$ with $v = 0.1$ V s^{-1}.

as the emitting layer (EML, 40 nm), and Alq_3 (10 nm) as the electron-transporting layer (ETL). LiF (0.5 nm) and Al (100 nm) were deposited as the cathode. The deposited film thickness was measured by a Tencor P-2 long scan profiler. The characteristics of the OLED device were measured using a Photoresearch PR650 spectrometer and a Keithley 306 source measure unit.

Preparation of 4,4-Dimethyl-2-(5-bromo-2-hydroxyphenyl)oxazoline (1). To a stirred solution of 5-bromo salicylic acid (4.34 g, 20 mmol) was added 2-amino-2-methyl-1-propanol (2.48 g, 20 mmol), PPh_3 (15.74 g, 3 equiv), and NEt_3 (8.32 mL, 3 equiv) in CH_2Cl_2 (100.0 mL), CCl_4 (19.30 mL, 10 equiv) dropwise via cannula at 0 °C for 8 h. The resulting solution was stirred at 50 °C for 12 h, after which the reaction mixture was cooled to room temperature and then dried under reduced pressure to give a pale yellow oil. The resulting residue was purified by silica gel column

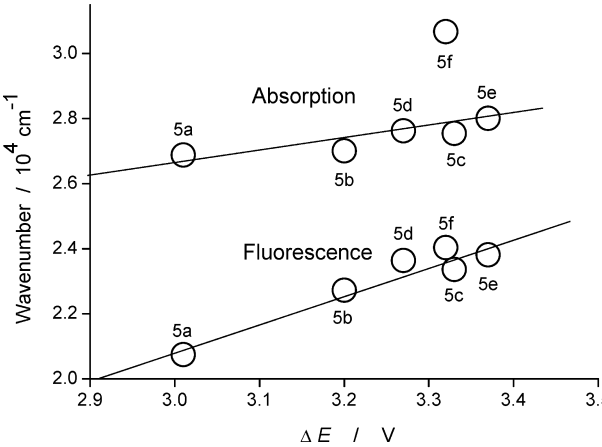

Figure 10. Plots of absorption and emission wavenumbers of Zn complexes (**5**) as a function of the ΔE ($= E_{pa1} - E_{pc1}$) values.

chromatography using hexane/benzene (*v*/*v* = 1/1) as an eluent to give a pale yellow oil **1** (2.70 g, 50%). ^{1}H NMR ($CDCl_3$): δ 12.22 (s, 1H, -O*H*), 7.79 (d, 1H, *Ph*, $J = 2.0$ Hz), 7.34 (dd, 1H, *Ph*, $J = 9.3$, 2.0 Hz), 6.77 (d, 2H, *Ph*, $^3J_{H-H} = 9.0$ Hz), 4.18 (s, 2H, -CH_2-), 1.36 (s, 6H, -CH_3). ^{13}C NMR ($CDCl_3$): δ 169.23, 167.48, 138.30, 131.99, 126.12, 110.46, 105.15, 78.13 (-*C*H_2-), 66.84, 28.44 (-*C*H_3). Anal. Calcd for $C_{11}H_{12}BrNO_2$: C, 48.91; H, 4.48. Found: C, 48.76; H, 4.45.

Synthesis of 4,4-Dimethyl-2-(5-bromo-2-benzyloxyphenyl)oxazoline (2). A mixture of 2-(5-bromo-2-hydroxyphenyl)oxazoline (**1**), K_2CO_3 (4.15 g, 30 mmol), and benzyl chloride (2.31 mL, 20 mmol) was dissolved in CH_3CN (100 mL) and refluxed for 12 h under nitrogen. After cooling to room temperature, methylene chloride was poured into the reaction mixture, and the solution was filtered through Celite. The volatile solvent was removed under reduced pressure, and the residue was purified by silica gel column chromatography using ethylacetate/hexane (*v*/*v* = 1/5) as an eluent to give **2** (2.88 g, 80%) as a white powder. TLC, $R_f = 0.7$. ^{1}H NMR ($CDCl_3$): δ 7.85 (d, 1H, *Ph*, $J = 2.4$ Hz), 7.43−7.30 (m, 5H, *Ph*), 7.28 (d, 1H, *Ph*, $J = 7.2$ Hz), 6.84 (d, 1H, *Ph*, $^3J_{H-H} = 9.0$ Hz), 5.11 (s, 2H, benzyl), 4.07 (s, 2H, -CH_2-), 1.38 (s, 6H, -CH_3). ^{13}C NMR ($CDCl_3$): δ 164.06, 160.03, 135.45, 135.21, 133.81, 129.02, 128.51, 128.44, 126.80, 115.53, 114.56, 79.12 (-*C*H_2-), 71.78, 70.89, 28.45 (-*C*H_3). Anal. Calcd for $C_{18}H_{18}BrNO_2$: C, 60.01; H, 5.04. Found: C, 60.07; H, 5.06.

Suzuki Coupling and Deprotection of the Benzyl Derivative by Hydrogenation. Synthesis of 4,4-Dimethyl-2-[5-(4-dimethylaminophenyl)-2-hydroxyphenyl]oxazoline (4a). 2-(5-Bromo-2-benzyloxyphenyl)oxazoline (3.6 g, 10 mmol), 4-dimethylaminophenylboronic acid (1.65 g, 10 mmol), K_3PO_4 (6.37 g, 30 mmol), palladium(II) acetate (0.13 g, 5 mol%), and tris(2-methoxyphenyl)phosphine (0.53 g, 15 mol%) were added to a two-phase mixture of dimethoxyethane (40 mL) and water (10 mL). The resulting

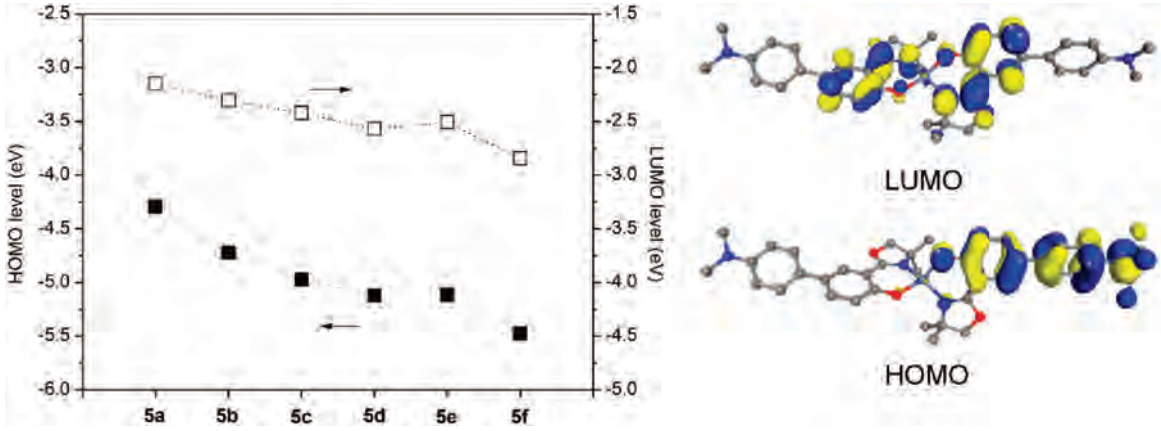

Figure 11. HOMO and LUMO energy levels (left) and orbital diagram (right) of **5** obtained by DMol^3 calculations.

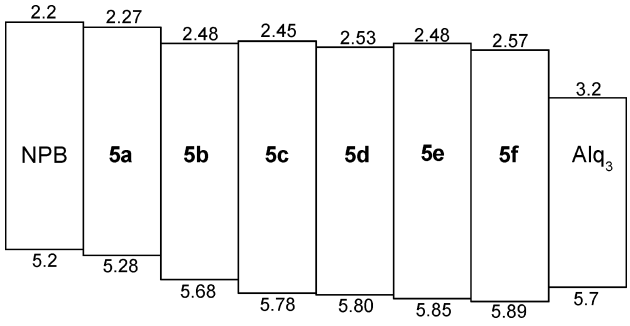

Figure 12. HOMO−LUMO levels of **5** estimated from cyclic voltammograms.

mixture was stirred under N_2 at 60 °C for 3 h. The mixture was hydrolyzed with water. The organic layer was extracted with CH_2Cl_2 (3 × 30 mL) and dried over magnesium sulfate. The solvent was removed under reduced pressure, and the residue was purified by silica gel column chromatography using benzene/hexane (1:1) as an eluent. **3a** was obtained as a pale yellow oil (2.00 g, 50%). The prepared benzyl-derivative **3a** with 10% Pd/C catalyst (1.0 g) was dissolved in 30 mL of THF/EtOH (1:1), and then, the mixture was shaken for 5 h under a hydrogen atmosphere (60 psi) at room temperature. The mixture was filtered through Celite to remove insoluble catalyst and dried under reduced pressure. The residue was purified by silica gel column chromatography using ethylacetate/hexane (v/v = 1/10) as an eluent to give **4a** as a yellow powder (1.35 g, 87%). ^{1}H NMR ($CDCl_3$): δ 12.14 (s, 1H, -O*H*), 7.82 (d, 1H, *Ph*, $^4J_{H-H}$ = 2.4 Hz), 7.57 (dd, 1H, *Ph*, $^3J_{H-H}$ = 8.4 Hz,$^4J_{H-H}$ = 2 Hz), 7.45 (d, 2H, *Ph*, $^3J_{H-H}$ = 8.8 Hz), 7.03 (d, 1H, *Ph*, $^3J_{H-H}$ = 8.4 Hz), 6.79 (d, 2H, *Ph*, $^3J_{H-H}$ = 8.8 Hz), 4.11 (s, 2H, -C*H*$_2$-), 2.98 (s, 6H, -NC*H*$_3$), 1.41 (s, 6H, -C*H*$_3$). ^{13}C NMR ($CDCl_3$): δ 163.71, 158.52, 149.76, 135.97, 132.11, 131.37, 127.34, 125.39, 117.07, 113.06, 111.14, 78.60 (-*C*H$_2$-), 67.41, 40.95 (-N*C*H$_3$), 28.85 (-*C*H$_3$). HRMS(FAB) calcd for $C_{19}H_{22}N_2O_2$: 310.1681. Found: 310.1695 [M]$^+$. Anal. Calcd for $C_{19}H_{22}N_2O_2$: C, 73.52; H, 7.14. Found: C, 73.48; H, 7.12.

Synthesis of 4,4-Dimethyl-2-[5-(4-methoxyphenyl)-2-hydroxyphenyl]oxazoline (4b). A procedure analogous to the preparation of **4a** was used but starting from 4-methoxyphenylboronic acid (1.52 g, 10 mmol). **4b** was obtained as a yellow, crystalline powder. Yield: 60% (1.78 g) based on 2-(5-bromo-2-benzyloxyphenyl)oxazoline. ^{1}H NMR ($CDCl_3$): δ 12.18 (s, 1H, -O*H*), 7.82 (d, 1H, *Ph*, $^4J_{H-H}$ = 2.4 Hz), 7.56 (dd, 1H, *Ph*,$^3J_{H-H}$ = 8.4 Hz, $^4J_{H-H}$ = 2.4 Hz), 7.48 (d, 2H, *Ph*, $^3J_{H-H}$ = 8.8 Hz), 7.05 (d, 1H, *Ph*, $^3J_{H-H}$ = 8.4 Hz), 6.95 (d, 2H, *Ph*, $^3J_{H-H}$ = 8.8 Hz), 4.11 (s, 2H, -C*H*$_2$-), 3.84 (s, 3H, -OC*H*$_3$), 1.41 (s, 6H, -C*H*$_3$). ^{13}C NMR ($CDCl_3$): δ

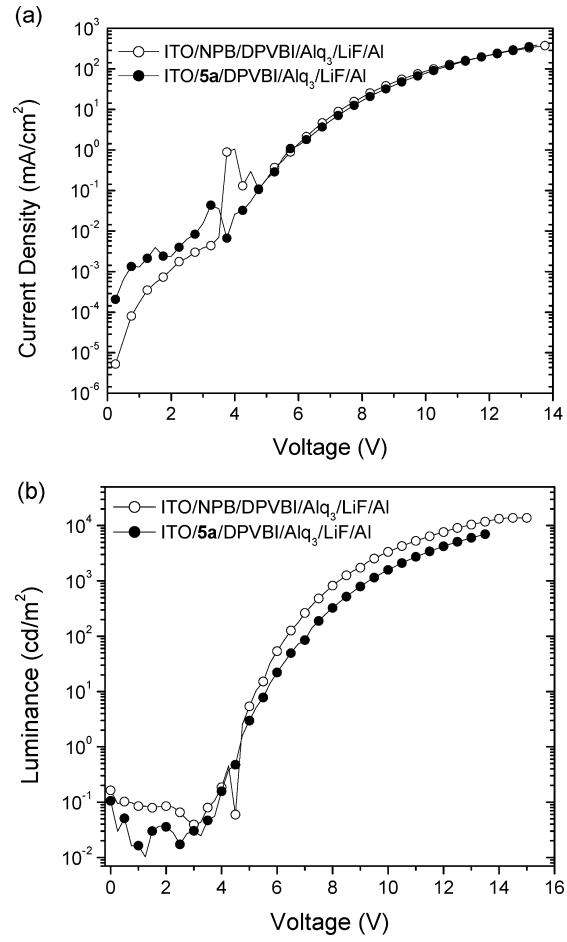

Figure 13. (a) I−V curve (current density vs voltage) and (b) L−V curve (luminance vs voltage) of ITO/NPB or **5a**/DPVBI/Alq$_3$/LiF/Al device.

163.60, 158.98, 158.86, 133.12, 131.68, 131.65, 127.78, 125.93, 117.19, 114.36, 111.20, 78.64 (-*C*H$_2$-), 67.45, 55.62 (-OC*H*$_3$), 28.83 (-*C*H$_3$). HRMS(FAB) calcd for $C_{18}H_{19}NO_3$: 297.1365. Found: 297.1378 [M]$^+$. Anal. Calcd for $C_{18}H_{19}NO_3$: C, 72.71; H, 6.44. Found: C, 72.67; H, 6.43.

Synthesis of 4,4-Dimethyl-2-[5-phenyl-2-hydroxyphenyl]oxazoline (4c). A procedure analogous to the preparation of **4a** was used but starting from phenyl boronic acid (1.22 g, 10 mmol). **4c** was obtained as a white powder. Yield: 75.6% (2.02 g) based on 2-(5-bromo-2-benzyloxyphenyl)oxazoline. ^{1}H NMR ($CDCl_3$): δ 12.22 (s, 1H, -O*H*), 7.88 (d, 1H, *Ph*, $^4J_{H-H}$ = 2.4 Hz), 7.58 (dd, 1H, *Ph*,$^3J_{H-H}$ = 8.4 Hz, $^4J_{H-H}$ = 2.4 Hz), 7.53 (d, 2H, *Ph*, $^3J_{H-H}$

Table 5. EL Spectral Data and Performance Characteristics of Devices

device	λ_{max} (nm)[a]	voltage (V)	current efficiency (cd/A)	luminance (cd/m^2)	max current efficiency (cd/A)	max luminance (cd/m^2)
ITO/NPB/**5c**/LiF/Al	431	7.6[b]	0.015[b]	23[b]	0.02	225
		12.1[c]	0.01[c]	127[c]		
ITO/NPB/**5c**/Alq_3/LiF/Al	428, 525	7.4[b]	0.7[b]	173[b]	0.8	3300
		9.5[c]	0.5[c]	1142[c]		
ITO/NPB/**5c**/BCP/Alq_3/LiF/Al	430	7.0[b]	0.24[b]	27[b]	0.3	1720
		11.4[c]	0.21[c]	376[c]		
ITO/**5a**/DPVBI/Alq_3/LiF/Al	446	7.5[b]	1.8[b]	180[b]	2.0	7000
		10.4[c]	1.9[c]	1650[c]		
ITO/NPB/DPVBI/Alq_3/LiF/Al	446	7.2[b]	3.3[b]	330[b]	3.5	13700
		10.1[c]	2.7[c]	3537[c]		

[a] Determined from the EL spectra. [b] @10 mA/cm^2. [c] @100 mA/cm^2.

= 7.2 Hz), 7.38 (t, 2H, *Ph*, $^3J_{H-H}$ = 7.6 Hz), 7.27 (t, 1H, *Ph*, $^3J_{H-H}$ = 7.2 Hz), 7.06 (d, 1H, *Ph*, $^3J_{H-H}$ = 8.4 Hz), 4.06 (s, 2H, -C*H*$_2$-), 1.37 (s, 6H, -C*H*$_3$). ^{13}C NMR ($CDCl_3$): δ 163.64, 159.54, 140.48, 132.08, 131.97, 128.99, 127.00, 126.80, 126.49, 117.34, 111.34, 78.67 (-*C*H$_2$-), 67.50, 28.86 (-*C*H$_3$). HRMS(FAB) calcd for $C_{17}H_{17}NO_2$: 267.1259. Found: 268.1343 $[M + H]^+$. Anal. Calcd for $C_{17}H_{17}NO_2$: C, 76.38; H, 6.41. Found: C, 76.35; H, 6.39.

Synthesis of 4,4-Dimethyl-2-[5-(4-chlorophenyl)-2-hydroxyphenyl]oxazoline (4d). A procedure analogous to the preparation of **4a** was used, but starting from 4-chlorophenyl boronic acid (1.56 g, 10 mmol). **4d** was obtained as a white, crystalline powder. Yield: 41% (1.24 g) based on 2-(5-bromo-2-benzyloxyphenyl)oxazoline. ^{1}H NMR ($CDCl_3$): δ 12.16 (s, 1H, -O*H*), 7.93 (d, 1H, *Ph*, $^4J_{H-H}$ = 2.4 Hz), 7.54 (dd, 1H, *Ph*,$^3J_{H-H}$ = 8.8 Hz, $^4J_{H-H}$ = 2.4 Hz), 7.44 (d, 2H, *Ph*, $^3J_{H-H}$ = 8.4 Hz), 7.36 (d, 2H, *Ph*, $^3J_{H-H}$ = 8.4 Hz), 7.01 (d, 1H, *Ph*, $^3J_{H-H}$ = 8.8 Hz), 4.06 (s, 2H, -C*H*$_2$-), 1.37 (s, 6H, -C*H*$_3$). ^{13}C NMR ($CDCl_3$): δ 170.11, 160.86, 140.14, 133.60, 132.63, 129.14, 128.16, 127.38, 124.37, 119.20, 117.03, 114.51, 71.01 (-*C*H$_2$-), 51.34, 30.40 (-*C*H$_3$). HRMS(FAB) calcd for $C_{17}H_{16}ClNO_2$: 301.0870. Found: 301.0856 $[M]^+$. Anal. Calcd for $C_{17}H_{16}ClNO_2$: C, 67.66; H, 5.34. Found: C, 67.68; H, 5.33.

Synthesis of 4,4-Dimethyl-2-[5-(2,4-fluorophenyl)-2-hydroxyphenyl]oxazoline (4e). A procedure analogous to the preparation of **4a** was used, but starting from 2,4-fluorophenyl boronic acid (1.58 g, 10 mmol). **4e** was obtained as a white powder. Yield: 64% (1.94 g) based on 2-(5-bromo-2-benzyloxyphenyl)oxazoline. ^{1}H NMR ($CDCl_3$): δ 12.31 (s, 1H, -O*H*), 7.78 (dd, 1H, *Ph*, $^5J_{H-F}$ = 1.0 Hz), 7.51 (ddd, 1H, *Ph*, $^5J_{H-F}$ = 1.0 Hz), 7.37 (d, 2H, *Ph*, $^3J_{H-H}$ = 8.4 Hz), 7.07 (d, 1H, *Ph*, $^3J_{H-H}$ = 8.8 Hz), 6.96−6.86 (m, 2H, *Ph*), 4.12 (s, 2H, -C*H*$_2$-), 1.41 (s, 6H, -C*H*$_3$). ^{13}C NMR ($CDCl_3$): δ 163.39, 159.60, 133.81, 131.23, 128.38, 125.53, 121.98, 117.08, 111.59, 104.51, 78.68 (-*C*H$_2$-), 67.49, 28.82 (-*C*H$_3$). HRMS(FAB) calcd for $C_{17}H_{15}F_2NO_2$: 303.1071. Found: 304.1161 $[M + H]^+$. Anal. Calcd for $C_{17}H_{15}F_2NO_2$: C, 67.32; H, 4.98. Found: C, 67.24; H, 4.95.

Synthesis of 4,4-Dimethyl-2-[5-(4-cyanophenyl)-2-hydroxyphenyl]oxazoline (4f). A procedure analogous to the preparation of **4a** was used, but starting from 4-cyanophenyl boronic acid (1.47 g, 10 mmol). **4f** was obtained as a white, crystalline powder. Yield: 42% (1.23 g) based on 2-(5-bromo-2-benzyloxyphenyl)oxazoline. ^{1}H NMR ($CDCl_3$): δ 12.40 (s, 1H, -O*H*), 7.70 (dd, 2H, *Ph*, $^3J_{H-H}$ = 8.4 Hz, $^4J_{H-H}$ = 2.0 Hz), 7.65 (dd, 2H, *Ph*, $^3J_{H-H}$ = 8.8 Hz, $^4J_{H-H}$ = 2.0 Hz), 7.62 (dd, 1H, *Ph*, $^3J_{H-H}$ = 8.4 Hz, $^4J_{H-H}$ = 2.0 Hz), 7.11 (d, 1H, *Ph*, $^3J_{H-H}$ = 8.8 Hz), 4.14 (s, 2H, -C*H*$_2$-), 1.43 (s, 6H, -C*H*$_3$). ^{13}C NMR ($CDCl_3$): δ 163.24, 160.52, 144.83, 132.77, 131.92, 129.67, 127.15, 126.77, 119.20, 117.75, 111.61, 110.43, 78.76 (-*C*H$_2$-), 67.60, 28.80 (-*C*H$_3$). HRMS(FAB) calcd for $C_{18}H_{16}N_2O_2$: 292.1212. Found: 293.1297 $[M + H]^+$. Anal. Calcd for $C_{18}H_{16}N_2O_2$: C, 73.95; H, 5.52. Found: C, 73.93; H, 5.51.

Preparation of the Zinc Complexes. Synthesis of Zinc(II) Bis{4,4-dimethyl-2-[5-(4-dimethylaminophenyl)-2-hydroxyphenyl]oxazolate} (5a). A solution of zinc acetate (0.183 g, 1 mmol) in EtOH (5.0 mL) was added dropwise to a solution of **4a** (0.620 g, 2 mmol) in EtOH (20.0 mL). After stirring at room temperature for 12 h, a white precipitate was filtered and washed with EtOH (2 × 5 mL). The washed product was recrystallized in CH_2Cl_2-hexane to give **5a** as a yellow, fine crystal. Yield: 87% (0.59 g). ^{1}H NMR ($CDCl_3$): δ 7.88 (s, 2H, *Ph*), 7.55 (dd, 2H, *Ph*, $^3J_{H-H}$ = 8.4 Hz, $^4J_{H-H}$ = 2.4 Hz), 7.44 (d, 4H, *Ph*, $^3J_{H-H}$ = 8.4 Hz), 6.92 (d, 2H, *Ph*, $^3J_{H-H}$ = 9 Hz), 6.78 (d, 4H, *Ph*, $^3J_{H-H}$ = 8.4 Hz), 4.17 (s, 4H, -C*H*$_2$-), 2.96 (s, 12H, -NC*H*$_3$), 1.39 (s, 12H, -C*H*$_3$). ^{13}C NMR ($CDCl_3$): δ 168.41, 149.35, 133.76, 127.33, 127.20, 126.92, 125.23, 123.63, 113.21, 109.00, 105.00, 78.02 (-*C*H$_2$-), 66.67, 40.96 (-N*C*H$_3$), 28.57 (-*C*H$_3$). HRMS(FAB) calcd for $C_{38}H_{42}N_4O_4Zn$: 682.2498. Found: 682.2474 $[M]^+$. Anal. Calcd for $C_{38}H_{42}N_4O_4Zn$: C, 66.71; H, 6.19. Found: C, 66.69; H, 6.17.

Synthesis of Zinc(II) Bis{4,4-dimethyl-2-[5-(4-methoxyphenyl)-2-hydroxyphenyl]oxazolate} (5b). A procedure analogous to the preparation of **5a** was used but starting from **4b** (0.59 g, 2 mmol). **5b** was obtained as a yellow crystal. Yield: 79% (0.52 g). ^{1}H NMR ($CDCl_3$): δ 7.91 (d, 2H, *Ph*, $^4J_{H-H}$ = 2.4 Hz), 7.55 (dd, 2H, *Ph*, $^3J_{H-H}$ = 8.4 Hz, $^4J_{H-H}$ = 2.8 Hz), 7.47 (d, 4H, *Ph*, $^3J_{H-H}$ = 8.8 Hz), 6.93 (d, 4H, *Ph*, $^3J_{H-H}$ = 8.8 Hz), 6.93 (d, 2H, *Ph*, $^3J_{H-H}$ = 10 Hz), 4.18 (s, 4H, -C*H*$_2$-), 3.82 (s, 6H, -OC*H*$_3$), 1.40 (s, 12H, -C*H*$_3$). ^{13}C NMR ($CDCl_3$): δ 169.64, 168.30, 158.35, 133.92, 133.69, 127.79, 127.30, 126.75, 123.76, 114.28, 109.07, 78.13 (-*C*H$_2$-), 66.82, 55.62 (-O*C*H$_3$), 28.73 (-*C*H$_3$). HRMS(FAB) calcd for $C_{36}H_{36}N_2O_6Zn$: 656.1865. Found: 656.1868 $[M]^+$. Anal. Calcd for $C_{36}H_{36}N_2O_6Zn$: C, 65.70; H, 5.51. Found: C, 65.48; H, 5.43.

Synthesis of Zinc(II) Bis{4,4-dimethyl-2-[5-phenyl-2-hydroxyphenyl]oxazolate} (5c). A procedure analogous to the preparation of **5a** was used but starting from **4c** (0.53 g, 2 mmol). **5c** was obtained as a white powder. Yield: 83% (0.50 g). ^{1}H NMR ($CDCl_3$): δ 7.98 (d, 2H, *Ph*, $^4J_{H-H}$ = 2.4 Hz), 7.61 (dd, 2H, *Ph*, $^3J_{H-H}$ = 8.6 Hz, $^4J_{H-H}$ = 2.8 Hz), 7.56 (d, 4H, *Ph*, $^3J_{H-H}$ = 7.2 Hz), 7.39 (t, 4H, *Ph*, $^3J_{H-H}$ = 8.0 Hz), 7.25 (t, 2H, *Ph*, $^3J_{H-H}$ = 7.6 Hz), 6.96 (d, 2H, *Ph*, $^3J_{H-H}$ = 8.8 Hz), 4.06 (s, 2H, -C*H*$_2$-), 1.37 (s, 6H, -C*H*$_3$). ^{13}C NMR ($CDCl_3$): δ 170.06, 168.31, 140.93, 134.13, 128.82, 128.41, 126.99, 126.27, 126.20, 123.85, 109.14, 78.15 (-*C*H$_2$-), 66.85, 28.75 (-*C*H$_3$). HRMS(FAB) calcd for $C_{34}H_{32}N_2O_4Zn$: 596.1654. Found: 596.1679 $[M]^+$. Anal. Calcd for $C_{34}H_{32}N_2O_4Zn$: C, 68.29; H, 5.39. Found: C, 68.21; H, 5.38.

Synthesis of Zinc(II) Bis{4,4-dimethyl-2-[5-(4-chlorophenyl)-2-hydroxyphenyl]oxazolate} (5d). A procedure analogous to the preparation of **5a** was used, but starting from **4d** (0.60 g, 2 mmol). **5d** was obtained as a white powder. Yield: 86% (0.57 g). ^{1}H NMR ($CDCl_3$): δ 7.94 (d, 2H, *Ph*, $^4J_{H-H}$ = 2.4 Hz), 7.55 (dd, 2H, *Ph*, $^3J_{H-H}$ = 8.4 Hz, $^4J_{H-H}$ = 2.4 Hz), 7.47 (d, 4H, *Ph*, $^3J_{H-H}$ = 8.4

Hz), 7.34 (d, 4H, *Ph*, $^3J_{H-H}$ = 8.4 Hz), 6.95 (d, 2H, *Ph*, $^3J_{H-H}$ = 8.8 Hz), 4.21 (s, 4H, -CH_2-), 1.42 (s, 12H, -CH_3). ^{13}C NMR ($CDCl_3$): δ 170.69, 168.16, 139.35, 133.86, 132.09, 128.92, 128.37, 127.47, 125.98, 123.95, 109.85, 78.20 (-*C*H_2-), 66.91, 28.69 (-*C*H_3). HRMS(FAB) calcd for $C_{34}H_{30}Cl_2N_2O_4Zn$: 664.0874. Found: 665.0935 $[M + H]^+$. Anal. Calcd for $C_{34}H_{30}Cl_2N_2O_4Zn$: C, 61.23; H, 4.53. Found: C, 61.17; H, 4.49.

Synthesis of Zinc(II) Bis{4,4-dimethyl-2-[5-(2,4-fluorophenyl)-2-hydroxyphenyl]oxazolate} (5e). A procedure analogous to the preparation of **5a** was used, but starting from **4e** (0.61 g, 2 mmol). **5e** was obtained as a white crystal. Yield: 89% (0.60 g). ^{1}H NMR ($CDCl_3$): δ 7.87 (s, 2H, *Ph*), 7.48 (d, 2H, *Ph*, $^3J_{H-H}$ = 8.4 Hz), 6.98 (d, 2H, *Ph*, $^3J_{H-H}$ = 8.8 Hz), 7.68−7.59 (m, 10H, *Ph*), 6.98 (d, 2H, *Ph*, $^3J_{H-H}$ = 8.8 Hz), 4.24 (s, 4H, -CH_2-), 1.44 (s, 12H, -CH_3). ^{13}C NMR ($CDCl_3$): δ 170.99, 168.06, 145.21, 133.77, 132.80, 132.69, 129.16, 126.46, 124.80, 124.31, 119.48, 109.43, 78.24 (-*C*H_2-), 67.01, 28.71 (-*C*H_3). (FAB) calcd for $C_{34}H_{28}F_4N_2O_4Zn$: 668.1277. Found: 668.1251 $[M]^+$. Anal. Calcd for $C_{34}H_{28}F_4N_2O_4Zn$: C, 60.95; H, 4.21. Found: C, 60.67; H, 4.17.

Synthesis of Zinc(II) Bis{4,4-dimethyl-2-[5-(4-cyanophenyl)-2-hydroxyphenyl]oxazolate} (5f). A procedure analogous to the preparation of **5a** was used, but starting from **4f** (0.58 g, 2 mmol). **5f** was obtained as a white powder. Yield: 91% (0.59 g). ^{1}H NMR ($CDCl_3$): δ 8.02 (d, 2H, *Ph*, $^4J_{H-H}$ = 2.4 Hz), 7.68−7.59 (m, 10H, *Ph*), 6.98 (d, 2H, *Ph*, $^3J_{H-H}$ = 8.8 Hz), 4.24 (s, 4H, -CH_2-), 1.44 (s, 12H, -CH_3). ^{13}C NMR ($CDCl_3$): δ 170.99, 168.06, 145.21, 133.77, 132.80, 132.69, 129.16, 126.46, 124.80, 124.31, 119.48, 109.43, 78.24 (-*C*H_2-), 67.01, 28.71 (-*C*H_3). HRMS(FAB) calcd for $C_{36}H_{30}N_4O_4Zn$: 646.1559. Found: 647.1626 $[M + H]^+$. Anal. Calcd for $C_{36}H_{30}N_4O_4Zn$: C, 66.72; H, 4.67. Found: C, 66.68; H, 4.65.

Crystal Structure Determination. Crystals of **5a**, **5b**, and **5e** were obtained from CH_2Cl_2/hexane (v/v = 2/1) and mounted on the diffractometer. Preliminary examination and data collection were performed using a Bruker SMART CCD detector system single-crystal X-ray diffractometer equipped with a sealed-tube X-ray source (40 kV × 50 mA) using graphite-monochromated Mo Kα radiation (λ = 0.71073 Å). Preliminary unit cell constants were determined from a set of 45 narrow-frame (0.3° in ω) scans. The double-pass method of scanning was used to exclude any noise. The collected frames were integrated using an orientation matrix determined from the narrow-frame scans. The SMART software package was used for data collection, and SAINT was used for frame integration.[20a] Final cell constants were determined by a global refinement of *xyz* centroids of reflections harvested from the entire data set. Structure solution and refinement were carried out using the SHELXTL-PLUS software package.[20b] Detailed information is listed in Table 1.

Acknowledgment. This work was supported by a grant (R02-2004-000-10095-0) from the Basic Research Program of the Korea Science and Engineering Foundation and a Korea University Grant of year 2003.

Supporting Information Available: ^{1}H and ^{13}C NMR spectroscopic data for **5**, cyclic voltammograms, UV−vis, and PL spectrums for **4** and **5**, orbital diagrams of **5** obtained by DMol^3 calculation, and EL properties of OLED devices using **5c** as an emitting layer (PDF); cif files for three crystal structures (**5a**, **5b**, and **5e**). This material is available free of charge via the Internet at http://pubs.acs.org.

IC702491J